IJIE

Journal homepage: http://penerbit.uthm.edu.my/ojs/index.php/ijie
ISSN : 2229-838X e-ISSN : 2600-7916

The International Journal of Integrated Engineering

Effects of Microstructure Architecture on the Fracture of Fibrous Materials

S. M. Chung, C. T. Koh*

Faculty of Mechanical and Manufacturing Engineering,
University of Tun Hussein Onn Malaysia, 86400 Parit Raja, Batu Pahat, Johor, MALAYSIA

*Corresponding author

DOI: https://doi.org/10.30880/ijie.2020.12.01.015
Received 5 May 2019; Accepted 8 December 2019; Available online 30 January 2020

Abstract: Fibrous materials is one of the potential scaffolds used for tissue engineered constructs. One of prerequisite properties for tissue engineered construct is fracture property. The work here study the relationship between microstructure architecture and fracture behavior of fibrous networks by using finite element analysis. The result shows that fibrous networks are toughened by either reducing the fiber density or cross-link percentage of networks. Such implementation increases the degree of non-affine deformation and produces a more compliant response at the crack-tip region. The non-affine deformation in fibrous networks involves fiber movement like fiber rearrangement and reorientation, where such mechanisms allow stress delocalization to occur at the crack-tip region and results in a better fracture toughness of fibrous networks. The findings form this work provide the design guideline of fibrous materials with enhanced toughness for multiple applications.

Keywords: Fracture, fibrous networks, fibrous materials

1. Introduction

Tissue engineering is one of the promising solutions for tissue reparation. In recent years, in-search of potential scaffolds used for tissue engineering constructs has been intensive. One example of tissue engineered scaffolds is an electrospun scaffold, which consists of the microstructure of fibrous scaffolds in the length scale of nano- and micro-meters. Electrospinning technique produces fibrous scaffold with different size and orientation of fibers through various treatment, set-up, spinning parameters and material solution [1-5]. The microstructure of scaffolds is often manipulated to satisfy the mechanical property and cell culture activities required from tissue engineering technique.

One of the major challenges encountered is to determine suitable microstructure architecture that satisfy both conditions [6]. A clear understanding between the microstructure architecture and mechanical properties of electrospun scaffolds helps in the design of fibrous materials. In the last decade, the approach to understand the mechanical behavior of fibrous materials has been intensive. These approaches are done by either experimental samples or computational models. The previous works show that the deformation of fibrous materials depends on both fiber properties and microstructure architecture of networks, *e.g.* fiber density, fiber diameter and cross-link density [7-14].

Unlike deformation, study on other mechanical property of fibrous materials is still lacking. One of the mechanical properties that required more understanding is fracture property. The fracture property of fibrous materials is vital, particularly in tissue engineering field due to the superior fracture toughness possessed by native tissue [6, 15]. Various studies show that the fracture behavior of fibrous materials is govern by the nonlinear zone that located at the near crack-tip region [16-18]. Further, these studies suggest that fiber properties and microstructure architecture like crosslink density are crucial on the fracture behavior of fibrous materials [17-19].

*Corresponding author: ctkoh@uthm.edu.my

The objective of this work is to present a more comprehensive study on the relationship of microstructure architecture (*i.e.* fiber density, fiber diameter and cross-link percentage) and fracture behavior of fibrous networks. The findings of this study lead to the production of fibrous materials with improved fracture toughness and refine the guideline for the design of fibrous materials.

2. Methodology

2.1 Modelling of finite element model

The fibrous network construction code was taken from previous work [18]. Fibrous networks were generated in MATLAB 2017b software by placing random line at random positions with random angles. These random lines were then extended to model boundary and were randomly bonded at the same node depending on user-defined cross-link percentage (*i.e.* the ratio between the sum of bonding points and the sum of fiber intersection points). The fiber density (*i.e.* the sum of fibers per unit area) and cross-link density (*i.e.* the sum of bonding points per unit area) of fibrous networks were calculated. The models were imported into finite element software, ABAQUS 2017 and were analyzed by using nonlinear finite element analysis, which considers large strain and rotation.

The effect of microstructure architecture on fracture behavior of fibrous networks were studied by constructing fibrous networks with various levels of fiber densities, fiber diameters and cross-link percentages. Fibrous networks were constructed with three levels of fiber density, 857.7 ± 3.9 mm^{-1}, 6521.2 ± 104.7 mm^{-1} and 67681.4 ± 902.1 mm^{-1}. The effect of cross-link percentage was studied by constructing these networks with cross-link percentage of 1 % to 100 % and with constant fiber diameter of 150 nm. The effect of fiber diameter was studied by modelling fibers with four levels of diameter, 50 nm, 150 nm, 500 nm and 1000 nm on fibrous networks with fiber density of 6521.2 ± 124.7 mm^{-1} and cross-link percentage of 6 %, 30 % and 100 %. The fibers were assigned with different fiber diameters. In addition, the fibers were defined with Young's modulus, E of 100 MPa and fracture strength, σ_f of 30 ± 4 MPa. The network configurations used are summarized in Table 1.

Table 1 - The network configurations used in this work

Case Study, (CS)	Circular Unit Size in Radius, (μm)	Fiber Density, ρ_f (mm^{-1})	Fiber ameter, Θ (nm)	Cross-link Percentage, (%)
1	1250	854.6 ± 8.5	150	1
2	1250	858.5 ± 1.9	150	15
3	1250	858.5 ± 1.9	150	30
4	1250	858.5 ± 1.9	150	75
5	1250	858.3 ± 2.2	150	100
6	75	6521.2 ± 124.7	50	6
7	75	6521.2 ± 124.7	150	6
8	75	6521.2 ± 124.7	500	6
9	75	6521.2 ± 124.7	1000	6
10	75	6521.2 ± 124.7	150	15
11	75	6521.2 ± 124.7	50	30
12	75	6521.2 ± 124.7	150	30
13	75	6521.2 ± 124.7	500	30
14	75	6521.2 ± 124.7	1000	30
15	75	6521.2 ± 124.7	150	50
16	75	6521.2 ± 124.7	150	75
17	75	6521.2 ± 124.7	50	100
18	75	6521.2 ± 124.7	150	100
19	75	6521.2 ± 124.7	500	100
20	75	6521.2 ± 124.7	1000	100
21	2.5	67792.3 ± 790.1	150	6

22	2.5	67733.7 ± 826.3	150	15
23	2.5	67584.0 ± 597.6	150	30
24	2.5	67609.3 ± 1145.7	150	50
25	2.5	68293.3 ± 918.5	150	75
26	2.5	67075.7 ± 1392.6	150	100

2.2 Fracture Analysis

The fibrous networks were constructed in circular unit with radius of 1250 µm, 75 µm and 2.5 µm depending on the fiber density of fibrous networks (Table 1) and the fibers were modelled by beam element, with the length of 10 µm, 1 µm and 0.1 µm, respectively. A notch was placed to each model with notch length that corresponds to its model's radius. The outer boundary of the models was subjected to the displacement field associated with the macroscopic crack-tip field for a homogeneous and isotropic material. The displacement components were calculated by refer to [2021]:

$$u_1 = \frac{1}{2}\sqrt{\frac{r}{2\pi}}\frac{K_1}{G}\left[\kappa - 1 + 2\sin^2\frac{\theta}{2}\right]\cos\frac{\theta}{2} \quad (1)$$

$$u_2 = \frac{1}{2}\sqrt{\frac{r}{2\pi}}\frac{K_1}{G}\left[\kappa + 1 - 2\cos^2\frac{\theta}{2}\right]\sin\frac{\theta}{2} \quad (2)$$

Where (u_1, u_2) are the displacements components in x- and y- axis, r is the length from origin of the notch to node, Θ is the angle between origin of the notch and node and K_1 is mode I stress intensity factor. Fibrous networks were assumed to experience plane stress condition, where $\kappa = (3\text{-}\nu)/(1+\nu)$ with Poisson's ratio, ν of 0.3 and shear modulus, G of 4 MPa [18]. Fibrous networks were assumed to be propagated once the first fibers exceeded fracture strength. The fracture of fibrous networks were then recorded and characterized by stress intensity factor (SIF).

3. Results

Fibrous networks were constructed with various levels of fiber densities, fiber diameters and cross-link percentages to study the effect of each microstructure property. Fig. 1(a) shows the effect of fiber diameter on stress intensity factor of fibrous networks. The result shows that fibrous networks modelled with different fiber diameters have similar fracture behavior with minor differences of stress intensity factor between them. The trend is consistent with three different levels of cross-link percentage. Further, fibrous networks with cross-link percentage of 6 % had larger standard deviation as compared to fibrous networks with higher cross-link percentage. Fig. 1(b) shows the effect of fiber density and cross-link percentage on stress intensity factor of fibrous networks. The result shows that stress intensity factor of fibrous networks increased with the decrease of fiber density. It was observed that sparse networks are possess with compliant response and a more homogeneous stress distribution at the crack-tip region through a series of fiber movement. The stress distribution became more confined as the fiber density increased due to limited fiber movement. On the other hand, the relationship between cross-link percentage and stress intensity factor of fibrous networks was nonlinear. It was found that the impact of cross-link percentage diminishes vastly after a cross-link percentage threshold of 30 %. The threshold value was consistent with three different network densities.

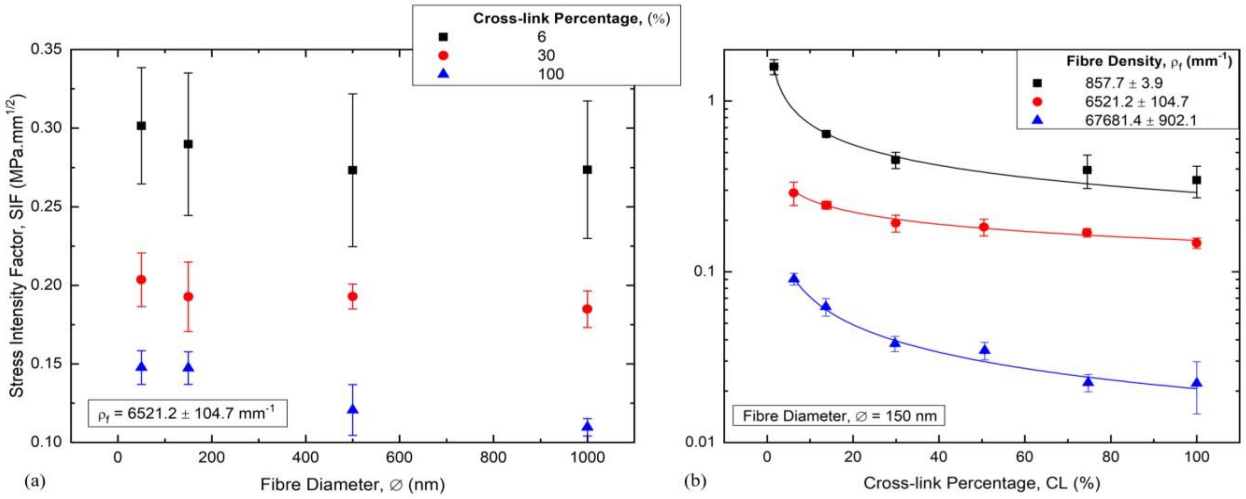

Fig. 1 - Stress intensity factor for fibrous networks constructed with (a) constant fiber density and different fiber diameter at various levels of cross-link percentages; (b) with constant fiber diameter and various levels of fiber densities at various levels of cross-link percentages

The fracture of fibrous networks with different fiber diameter shows that the stress distribution at the crack-tip region are affected by the fiber diameter. Fig. 2 shows fibrous network with fiber diameter of 150 nm has a more homogeneous stress distribution as compared to fibrous network with fiber diameter of 500 nm. The changes of stress distribution at the crack-tip region is attributed to the buckling ability of fibers that are dependent on its diameter. Since the fibers are easily bend then stretch, the buckling ability of fibers affect the fiber rearrangement and reorientation at the crack-tip region, resulting a different stress distribution as well as different failure location. Fig. 3 shows the fracture behavior of fibrous networks that constructed with different levels of cross-link percentage. The result shows that fibrous network with cross-link percentage of 6 % has a more homogeneous stress distribution and blunted cracktip. As the cross-link percentage increased to 15 %, the stress distribution became more concentrated and still posses with blunted crack-tip. While fibrous networks with cross-link percentage of 30 % to 100 % have stress confined at a very small region and sharp crack-tip. The different fracture behavior shown by these fibrous networks are attributed to the cross-link density, where it act as constraints for fiber rearrangement and reorientation. The fiber rearrangement and reorientation at the crack-tip region are found to have significant impact on the stress distribution and crack opening.

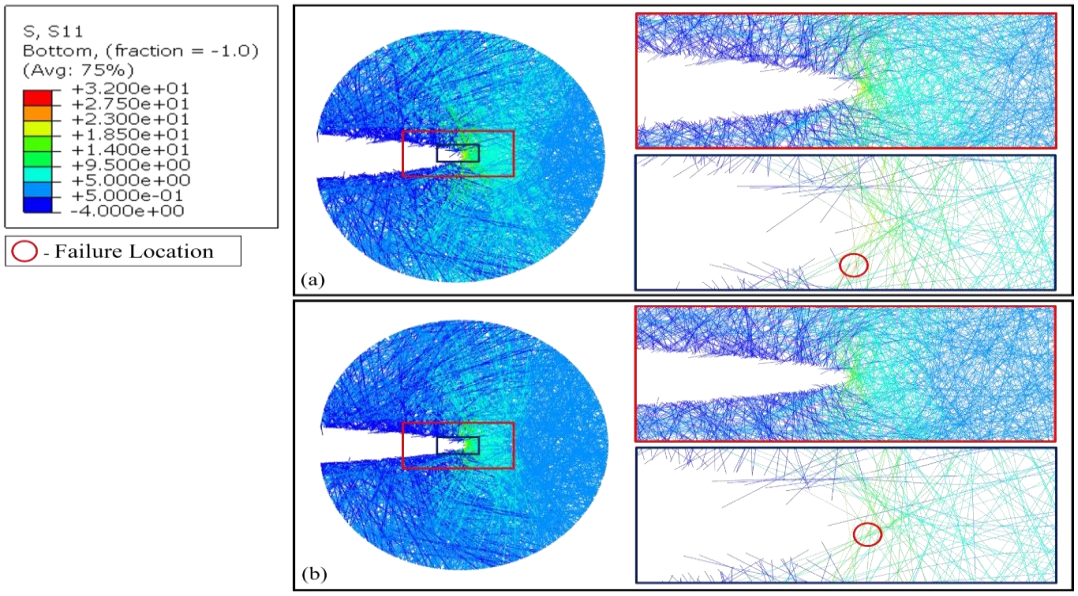

Fig. 2 - The effect of fiber diameters on stress distribution of fibrous networks showing different stress distribution, critical locations and crack tip opening. Two levels of fiber diameters, (a) 150 nm and (b) 500 nm are assigned on fibrous network constructed with fiber density of 6651.9 mm^{-1} and cross-link percentage of 6 %

4. Discussion

The work here suggests that the dominant microstructure property that affects fracture behavior of fibrous networks are fiber density and cross-link percentage. Fibrous networks were toughened by either reducing fiber density or cross-link percentage of networks. These microscopic parameters affect non-affine deformation. Non-affine deformation in fibrous networks involved fiber movement including fiber rearrangement and reorientation. In this study, the degree of non-affine deformation was represented by key parameter, L_c/ρ_f. The parameter L_c, contour length was defined as the fiber length between two cross-linked points [18] while ρ_f refers to the fiber density of fibrous networks. A master curve is obtained by plotting the graph of stress intensity factor and L_c/ρ_f (Fig. 4).

The parameter, L_c/ρ_f describes the length of fiber that is constrained at both ends and its arrangement within the network. The parameter, Lc represents the cross-link density and buckling ability of fiber. With large contour length, fibers are expected to bend easily and have frequent fiber-fiber sliding due to lesser constraints. This results in a greater amount of fiber movement and produces a more homogeneous stress distribution at the crack-tip region. The movement of fibers allow crack to blunt instead of propagate, where stress delocalization occurs at the crack-tip region [16, 18]. Such mechanisms toughen the fibrous networks. The parameter, ρ_f on the other hand is an indication on the frequency of fiber overlapping within fibrous networks. It is noticed that fibrous networks could possess similar contour length by different network configurations (*e.g.* altering cross-link percentage and fiber density of fibrous networks). The fiber density reflects on how these fibers are arranged within the network. Dense networks have fibers that are frequently connected to each other as compared to sparse fibrous network, resulting in more constraints that limit the fiber movement. Thus, dense fibrous networks are found to have poorer fracture toughness compared to sparse fibrous networks.

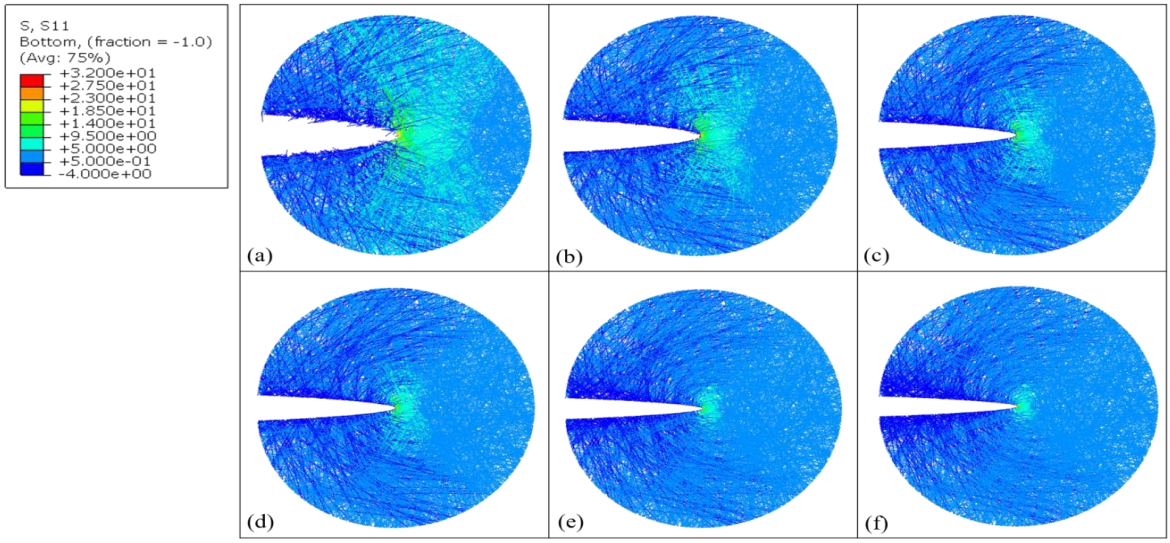

Fig. 3 - The stress distribution for fibrous networks constructed with fiber density of 6651.9 mm^{-1} and cross-link percentage of (a) 6 %, (b) 15 %, (c) 30 %, (d) 50 %, (e) 75 % and (f) 100 %

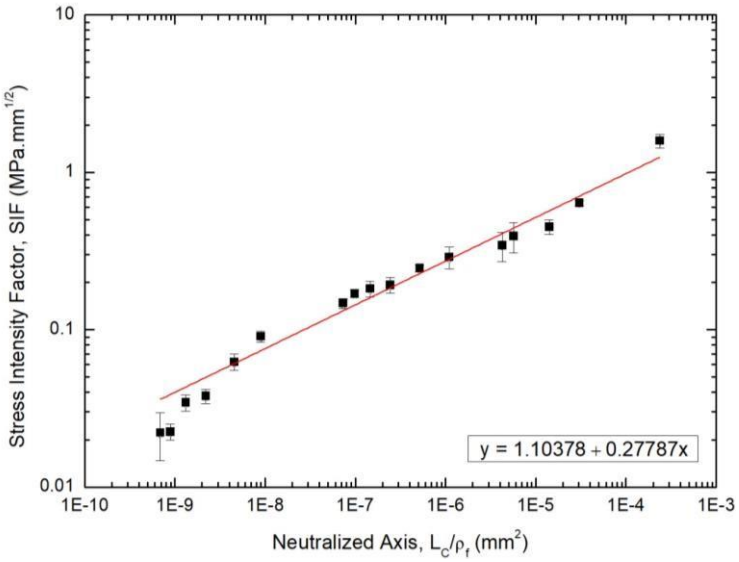

Fig. 4 - The relationship of stress intensity factor and normalized axis, L_c/ρ_f for fibrous networks

5. Conclusion

Fracture property is one of prerequisite properties for tissue engineered construct. Our work shows that the fracture behavior of fibrous networks are dependent on fiber density and cross-link percentage of networks. Fibrous networks are toughened by either reducing the fiber density or cross-link percentage of networks. Such implementation increases the degree of non-affine deformation of fibrous networks. The non-affine deformation in fibrous networks refers to fiber movement involving fiber rearrangement and reorientation. The fiber kinematic allows stress delocalization to occur at the crack-tip region and produces a more homogeneous stress distribution. Such mechanisms toughen fibrous networks and prevent it from crack propagation. In addition, the degree of non-affine deformation is represented by a key parameter, L_c/ρ_f. The work here presents a comprehensive study on the relationship of microstructure architecture and fracture behavior of fibrous networks. This helps to refine the guideline for the design of fibrous materials and allow the use of fibrous materials in multiple applications including tissue engineering and textile application.

Acknowledgement

The authors would like to express their gratitude to University of Tun Hussein Onn Malaysia [GPPS/U807], Ministry of Science, Technology and Innovation Malaysia [03-01-13-SF0112-S026] and the Ministry of Education Malaysia [FRGS/1/2014/TK01/UTHM/02/2-1462] for funding the research work.

References

[1] W. Khoo and C. T. Koh, "A review of electrospinning process and microstructure morphology control," *ARPN J. Eng. Appl. Sci.*, vol. 11, no. 12, pp. 7774–7781, 2016.

[2] V. Thomas, M. V Jose, S. Chowdhury, J. F. Sullivan, D. R. Dean, and Y. K. Vohra, "Mechano-morphological studies of aligned nanofibrous scaffolds of polycaprolactone fabricated by electrospinning," *J. Biomater. Sci. Polym.*, vol. 17, no. 9, pp. 969–984, 2006.

[3] N. Okutan, P. Terzi, and F. Altay, "Affecting parameters on electrospinning process and characterization of electrospun gelatin nanofibers," *Food Hydrocoll.*, vol. 39, pp. 19–26, 2014.

[4] J. M. Deitzel, J. Kleinmeyer, D. Harris, and N. C. Beck Tan, "The effect of processing variables on the morphology of electrospun nanofibers and textiles," *Polymer (Guildf).*, vol. 42, no. 1, pp. 261–272, 2001.

[5] S. Soliman, S. Sant, J. W. Nichol, M. Khabiry, E. Traversa, and A. Khademhosseini, "Controlling the porosity of fibrous scaffolds by modulating the fiber diameter and packing density," *J. Biomed. Mater. Res. A*, vol. 96, no. 3, pp. 566–574, 2011.

[6] D. W. Hutmacher, "Scaffolds in tissue engineering bone and cartilage," *Biomaterials*, vol. 21, pp. 2529–2543, 2000.

[7] Y. Yin and J. Xiong, "Finite element analysis of electrospun nanofibrous mats under biaxial tension," *Nanomaterials*, vol. 8, no. 5, p. 348, 2018.

[8] Y. Yin, Z. Pan, and J. Xiong, "A tensile constitutive relationship and a finite element model of electrospun nanofibrous mats," *Nanomaterials*, vol. 8, no. 1, p. 29, 2018.

[9] T. Stylianopoulos, C. A. Bashur, A. S. Goldstein, S. A. Guelcher, and V. H. Barocas, "Computational predictions of the tensile properties of electrospun fiber meshes: effect of fibre diameter and fibre orientation," *J. Mech. Behav. Biomed. Mater.*, vol. 1, no. 4, pp. 326–335, 2008.

[10] F. Croisier, A. S. Duwez, C. Jérôme, A. F. Léonard, K. O. Van der Werf, P. J. Dijkstra, and M. L. Bennink, "Mechanical testing of electrospun PCL fibers," *Acta Biomater.*, vol. 8, no. 1, pp. 218–224, 2012.

[11] C. Xiang and M. W. Frey, "Increasing mechanical properties of 2-D-structured electrospun nylon 6 non-woven fiber mats," *Materials (Basel).*, vol. 9, no. 4, Apr. 2016.

[12] X. Mao, "Mechanics of disordered fiber networks," *in Gels and Other Soft Amorphous Solids*, 2018, pp. 199–210

[13] S. C. Wong, A. Baji, and S. Leng, "Effect of fiber diameter on tensile properties of electrospun poly (εcaprolactone)," *Polymer (Guildf).*, vol. 49, no. 21, pp. 4713–4722, 2008.

[14] C. T. Koh, C. Y. Low, and Y. Yusri, "Structure-property relationship of bio-inspired fibrous materials," *Procedia Comput. Sci.*, vol. 76, pp. 411–416, 2015.

[15] A. Baji, Y. W. Mai, S. C. Wong, M. Abtahi, and P. Chen, "Electrospinning of polymer nanofibers: effects on oriented morphology, structures and tensile properties," *Compos. Sci. Technol.*, vol. 70, no. 5, pp. 703–718, 2010.

[16] U. Stachewicz, I. Peker, W. Tu, and A. H. Barber, "Stress delocalization in crack tolerant electrospun nanofiber networks," *ACS Appl. Mater. Interfaces*, vol. 3, no. 6, pp. 1991–1996, 2011.

[17] C. T. Koh and M. L. Oyen, "Toughening in electrospun fibrous scaffolds," *APL Mater.*, vol. 3, p. 14908, 2015.

[18] C. T. Koh and M. L. Oyen, "Branching toughens fibrous networks," *J. Mech. Behav. Biomed. Mater.*, vol. 12, pp. 74–82, 2012.

[19] X. Wei, Z. Xia, S. C. Wong, and A. Baji, "Modelling of mechanical properties of electrospun nanofibre network," *Int. J. Exp. Comput. Biomech.*, vol. 1, no. 1, p. 45, 2009.

[20] M. F. Kanninen and C. H. Popelar, *Advanced fracture mechanics*. 1st Edition, Oxford University Press, 1985.

[21] A.E Ismail, A.K Ariffin, S. Abdullah, M.J Ghazali. "Finite element analysis of J-integral for surface cracks in round bars under combined mode I loading", International Journal of Integrated Engineering, vol. 9, no. 2. 1-8. 2017.

[22] A.E Ismail, S. Jamian, KA Kamarudin, M.K.M Nor, M.N Norihan, M.A Choiron. "An overview of fracture mechanics with ANSYS", International Journal of Integrated Engineering, vol. 10, no. 5, 59-67, 2018.